Measurement of the Ly-α Mg resonance with the $2s \rightarrow 3p$ Ne-like Ge line

Joseph Nilsen, Peter Beiersdorfer, Steven R. Elliott, and Thomas W. Phillips
Lawrence Livermore National Laboratory, L-59, Livermore, California 94550

B. A. Bryunetkin, V. M. Dyakin, T. A. Pikuz, and A. Ya. Faenov
National Scientific and Research Institute for Physical-technical and Radio-technical Measurements, Mendeleevo, 141570 Moscow Region, Russia

S. A. Pikuz
P. N. Lebedev Physical Institute, Russian Academy of Sciences, Moscow 117924, Russia

S. von Goeler and M. Bitter
Princeton Plasma Physics Laboratory, Princeton, New Jersey 08543

P. A. Loboda, V. A. Lykov, and V. Yu. Politov
National Institute of Technical Physics, P.O. Box 245, Chelyabinsk-70, 454070, Russia
(Received 30 March 1994)

Measurements and calculations of the resonance between the Ly-α line of magnesium and the $2s \rightarrow 3p$ transition in neonlike germanium are presented. This resonance is of possible use as part of a resonantly photo-pumped x-ray laser scheme recently proposed which would lase on several $2p \rightarrow 2s$ transitions between 64 and 89 Å in neonlike germanium. Measurements of the resonance are made by three different approaches: one using the electron beam ion trap, the second using laser-produced plasma, and the third on a tokamak. These results are compared with calculations and other measurements. Certain discrepancies are observed with previous measurements which may be due to the partial overlap between oxygenlike and neonlike lines in germanium. The results do show a good resonance between magnesium and germanium, with the germanium line between the two Ly-α components of magnesium but nearer to the short-wavelength component.

PACS number(s): 32.30.Rj, 42.60.By

I. INTRODUCTION

Many scientists over the last 15 years have proposed different x-ray-laser schemes which use the resonant photo-pumping mechanism, in the hope of developing a high-efficiency x-ray laser [1,2]. Currently most x-ray lasers use either collisional excitation or recombination as the pumping mechanism [1–3]. An important requirement and difficulty of the resonant photo-pumping approach is the need for two ions with a good resonance between a strong pump line and an absorbing line which feeds the lasing transition. Usually, calculations are not accurate enough to predict the resonances to the few hundred parts per million (ppm) accuracy required. Only recently have experiments started to routinely do measurements with this accuracy to verify potential resonances [4–7]. These measurements are proving invaluable in the effort to improve the atomic physics calculations and decide which x-ray laser schemes to pursue experimentally.

This paper presents measurements of the resonance required for a recently proposed [8,9] x-ray laser scheme which would lase on several $2p \rightarrow 2s$ transitions in neonlike germanium ($Z=32$) and which is resonantly photo-pumped by Ly-α radiation from hydrogenlike magnesium ($Z=12$). The basic lasing scheme, shown in Fig. 1, uses the Mg Ly-α, $2p \rightarrow 1s$, emission lines to radiatively pump an electron in the ground state of the Ne-like Ge ion to the $\overline{2s}_{1/2}3p_{1/2}$ ($J=1$) upper laser state. This state decays directly to the $\overline{2p}_{3/2}3p_{1/2}$ ($J=2$) state, which is the lower laser state for the 64-Å laser transition. The other laser

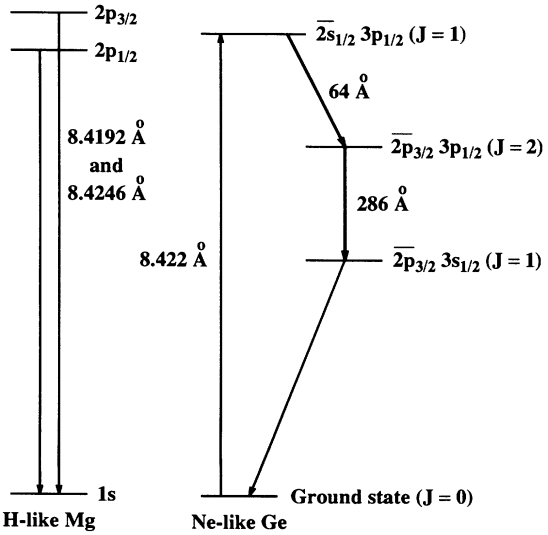

FIG. 1. Energy-level diagram showing the resonant photo-pumping mechanism for the 64 Å Mg-pumped Ge X-ray laser transition.

lines have different lower states. The bar over the $2s$ and $2p$ states indicate a hole or vacancy in the closed L shell [$1s^2 2s^2 2p^6$] or neonlike core. Therefore, lasing can be thought of as taking place between holes in a closed L shell. This is equivalent to lasing from $2p \rightarrow 2s$. In addition, the $\overline{2p_{3/2}} 3p_{1/2}$ ($J=2$) state is the upper laser state for the observed $3p \rightarrow 3s$ laser transition at 286 Å [1,2]. The details of this scheme are discussed in Refs. [8] and [9].

The measurements were done by three methods. The first used the electron beam ion trap (EBIT) at Lawrence Livermore National Laboratory (LLNL), the second measured the spectra in laser-produced plasmas at the National Scientific and Research Institute for Physical-technical and Radio-technical Measurements (NPO VNIIFTRI) laser facility, and the third recorded data from the Princeton Large Torus (PLT) tokamak.

II. EBIT MEASUREMENTS

EBIT uses an electron beam to generate, trap, and excite highly charged ions in a 2-cm long trapping region, as described in detail by Marrs, Levine, and co-workers [10,11]. The energy of the electron beam can be varied between 500 and 40 000 eV to select the ionization state of interest. The full width at half maximum (FWHM) width of the beam energy is about 50 eV. This allows EBIT to isolate different ionization stages. We will show that this is an important feature when different ionization stages have lines of similar wavelength. Figure 2 shows the calculated charge-state population versus beam energy for Ge. Below 2.18 keV, almost all the population is in the Ne-like Ge sequence, as expected for a beam energy below the ionization potential of Ne-like Ge. As the beam energy is increased the different charge states are produced. By operating the beam energy just below the ionization potential of a particular ionization state, higher charge states can be avoided. The ionization potentials are 2.18, 2.30, 2.43, and 2.56 keV for Ne-like, F-like, O-like, and N-like Ge, respectively. The beam current for the Ge measurements was 86 mA. The beam energy and current for the Mg measurements was 4.0 keV and 120 mA, respectively.

The beam energy is a sum of two contributions; the trap electrode–electron gun voltage difference and a contribution due to the space charge of the beam. The space charge contribution at this beam current decreases the beam energy by an estimated 50 eV. The exact value of the space charge has not been measured in these experiments. In order to provide data to deduce the spectral contributors from the various charge states, Ge spectra were taken for trap electrode–electron gun voltage differences of 2.02, 2.23, 2.28, 2.36, 2.41, 2.49, 2.55, and 2.66 keV. Figure 3 shows Ge spectra at beam energies of 2.02, 2.36, and 2.41 keV. At 2.02 keV, the spectrum is Ne-like Ge with the transitions from $\overline{2s_{1/2}} 3p_{3/2}$ ($J=1$) and $\overline{2s_{1/2}} 3p_{1/2}$ ($J=1$) to the ground state, referred to as $3A$ and $3B$, respectively, visible near 8.4 Å. As the beam energy is raised to 2.36 keV, the Ne-like features become smaller and strong F-like features appear between 8.5 and 8.6 Å. A small amount of O-like features are also begin-

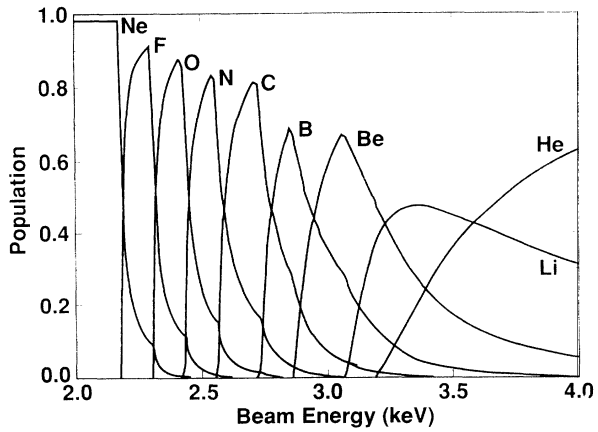

FIG. 2. Calculated population of the various isoelectronic sequences of Ge versus the EBIT beam energy. Below a beam energy of 2.18 keV almost all the population is in the Ne-like Ge charge state.

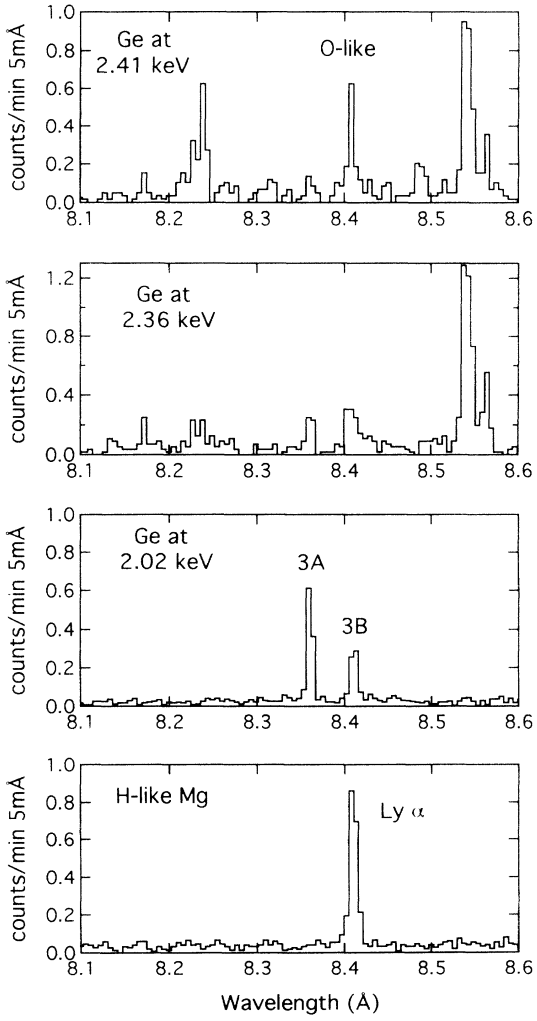

FIG. 3. Spectra of Ge taken at various beam energies on EBIT. The Mg spectra is used to calibrate the wavelength and shows the good resonance between the Ne-like Ge line $3B$ and the Ly-α Mg line near 8.42 Å.

ning to show at this energy. Finally, with the beam energy at 2.41 keV, the Ne-like features disappear and O-like lines appear near 8.2 and 8.4 Å, while the F-like features remain strong. The O-like Ge line at 8.4 Å, identified as the $(2p_{3/2})^3 3d_{5/2}(J=3) \rightarrow (2p_{3/2})^2(J=2)$ transition, is of particular importance because of its near coincidence with $3B$, the line of interest. In situations where the Ne-like and O-like charge states coexist, the lines are blended and cannot be resolved. The present measurements allowed us to distinguish between $3B$ and the O-like line because of the charge-state selectivity afforded by the electron beam as predicted in Fig. 2 and illustrated in Fig. 3.

Because the lines of interest are in the soft-x-ray region we used an evacuated crystal spectrometer for our measurements. To record the data in Fig. 3, a flat crystal spectrometer with a thallium hydrogen phthalate (TlAP) crystal ($2d=25.9$ Å) in second order was used. The spectrometer employed a position-sensitive proportional counter filled with 1 atm of P-10 (90% argon, 10% methane) [12]. The 8×50 mm^2 entrance window consists of a 4-μm thick polypropylene foil which allowed detection of photons down to 650 eV. The spectrometer vacuum (10^{-6} torr) was separated from EBIT's main vacuum chamber (10^{-10} torr) by a 1-μm thick polyimide foil. The resolving power of the crystal and the spatial resolution of the detection limit the spectral resolving power to approximately $\lambda/\Delta\lambda=2000$. A more detailed description of the spectrometer is given in Ref. [12]. The metallic elements were injected into the trap with a metal vacuum vaporization arc source as described in Ref. [13].

Measurements of the Mg and Ge resonance were made sequentially. Recording a single spectrum required about 20 min. To verify the absence of drift in the experiments, several runs were done alternating between the two materials. The Mg Ly-α_1 and Ly-α_2 lines are used as absolute reference lines with values of 8.419 20 Å (1472.64 eV) and 8.424 61 Å (1471.69 eV) based on theoretical calculations [14–18]. These lines were not resolved so the best fit to the shape of the Ly-α line, which resulted in a 60-40 % split between the two Ly-α components, was used to calibrate the spectra. The resolution was 0.76 eV FWHM and the two components were separated by 0.95 eV. The dispersion was determined by assuming a 9.3 eV separation between the Ne-like Ge ground state to $2s_{1/2}3p_{3/2}$ $(J=1)$ and $2s_{1/2}3p_{1/2}$ $(J=1)$ transitions as calculated with the multiconfiguration Dirac-Fock (MCDF) atomic physics code of Grant and co-workers [19] in the average level (AL) mode. A systematic uncertainty arose due to the determination of the estimated dispersion. The separation of $3A$ and $3B$ is 9.3±0.5 eV, where the 0.5 eV represents the theoretical uncertainty. Because line $3B$ is near the Ly-α calibration line, this results in a small contribution to the uncertainty in the line position, about 0.01 eV. By adjusting the EBIT beam energy to optimize the Ne-like charge state, we measured a separation of 0.48 eV between Mg Ly-α_1 and the Ne-like Ge $3B$ line. This gives a value of 8.4219 Å±1.0 mÅ (1472.16±0.18 eV) for the $3B$ line. By raising the beam energy to produce O-like Ge, we measured the separation of the O-like Ge $2p \rightarrow 3d$ line from Mg Ly-α_1 to be 0.07 eV, which results in a value of 8.4188 Å±1.1 mÅ (1472.71 ±0.19 eV) for the O-like Ge $2p \rightarrow 3d$ line. In jj coupling this O-like Ge line is the $(2p_{3/2})^2(J=2) \rightarrow (2p_{3/2})^3 3d_{5/2}(J=3)$ transition. The experiments measured the values in wavelength and we used $hc=12\,398.42$ eV Å to convert to energy. The uncertainties in the Ge line positions were due to a combination of the statistical uncertainties in determining the centroid of the Ge line and a 0.1 eV contribution from the uncertainty in the centroid of the Mg line depending on what assumptions were made about the blend of the two components.

A second set of measurements was done with EBIT using an ammonium dihydrogen phosphate (ADP) crystal ($2d=10.648$ Å) in first order and gave 8.4208 Å±0.8 mÅ (1472.35±0.14 eV) for the $3B$ line. These measurements were of somewhat lower resolution but had better statistics and gave results consistent with the previous measurements

III. VNIIFTRI MEASUREMENTS

The second set of measurements was done on a laser produced plasma at the NPO VNIIFTRI laser facility. Figure 4 shows the experimental setup. A Nd laser with up to 30 J of energy with a pulse duration of 2 ns was focused to a 100-μm diameter spot onto a solid sample of Mg or Ge. Three different types of targets were used: single targets of Mg or Ge; compound targets with samples of Mg and Ge adjacent in a single plane; and compound targets which had Ge and Mg adjacent but in different planes with the Ge target surface 200 μm above the Mg surface. Two different types of spectrographs were used to record the data on direct exposure film (DEF-2). One spectrograph used a flat CsAP (cesium biphthalate) crystal ($2d=26.1$ Å) with a 150-μm-wide slit which was placed parallel to the surface of the target so as to allow spatial resolution perpendicular to the target in the direction of the expanding plasma. The second spectrograph

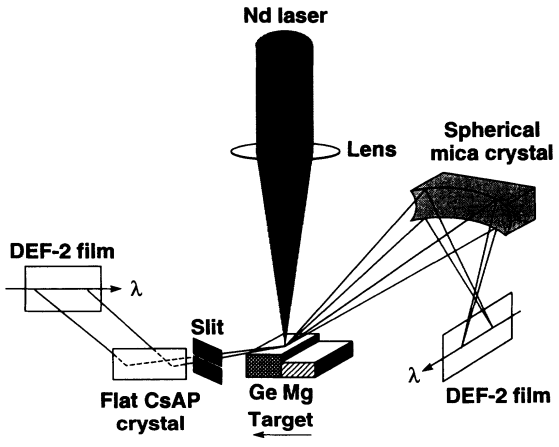

FIG. 4. Experimental geometry for the spectral measurements done at the NPO VNIIFTRI laser facility. A Nd laser illuminates a Ge or Mg target. Spectra are recorded with flat and curved crystal spectrographs. The curved crystal spectrograph uses the geometry of the focusing spectrograph with spatial resolution (FSSR).

used a spherical mica crystal ($2d = 19.944$ Å in second order) bent to a radius of 100 mm. This spectrograph was placed in the geometry of the focusing spectrograph with spatial resolution (FSSR) [20,21]. In this case, one direction provided spectral resolution as in the Johann type spectrographs while the perpendiuclar direction provided spatial resolution. The spatial resolution was in the direction of the expanding plasma. The target was outside the Rowland circle at a distance of 194 mm from the crystal. The film was located 85 mm from the crystal and second order diffraction is used. The Bragg angle was approximately 58°. For this geometry, the distance between the source and crystal is $-R\sin\theta/\cos 2\theta$, the distance from the crystal to film is $R\sin\theta$, the magnification is $-\cos 2\theta$ where θ is the Bragg angle such that $2d\sin\theta = n\lambda$ and R is the radius of curvature of the crystal. The radius of the Rowland circle is $R/2$. This spectrograph geometry allowed us a unique combination of very good spectral resolving power, $\lambda/\Delta\lambda$, of 6000 in this experiment and as much as 10 000 in other experiments [22], good spatial resolution of 20–30 μm, and very high brightness for recording data on film.

Spectra were recorded on both spectrographs using the three types of targets described above. The spectra from the flat-crystal spectrograph covered a large spectral range and while it has inadequate spectral resolution to measure the resonance to the required accuracy it does show that there is a near resonance worth measuring at higher resolution. The spectra from the FSSR spectrograph have spatial resolution in the direction of the expanding plasma and good spectral resolution which enables us to resolve the line structure near Ly-α Mg and the Ne-like Ge lines. Near the surface of the target, even the good spectral resolution does not help to resolve the Ly-α components because of the large linewidths. As was shown in Ref. [23], the widths of the lines become much narrower far from the target surface and are limited by the rocking curve of the crystals. Using a spherical mica crystal with extremely small bending radius allowed us to register the spectra of the Mg and Ge plasmas from coronal regions of the expanding plasmas. In this region, the Ly-α components are resolved. This greatly improves the absolute calibration of the system. These data yields a value of 8.4208 Å$\pm$0.9 mÅ for the Ge $3B$ line using the absolute values of the Ly-α components as reference lines.

To try and improve the resolution additional measurements were done with the FSSR spectrograph using a larger radius crystal ($R = 250$ mm). Figure 5 presents the film density of the Mg and Ge spectra measured in the coronal region using this spectrograph. As usual, the spectra were taken in two shots, one shot for Mg followed by a second shot in which the Ge was moved into the laser focus. In this case, we recorded two spectra on one film. By measuring the coronal region we can isolate the Ne-like Ge lines from the O-like Ge lines which tend to be more present in the higher temperature and density region near the target surface. As discussed before, the absolute values of the Ly-α components are used as reference lines. Doing this, the $2s \rightarrow 3p$ Ne-like Ge line $3B$ is measured at 8.4209 Å$\pm$0.8 mÅ. As with the EBIT measurements, the higher resolution traded off against poorer statistics and the resulting uncertainty is about the same as given above for the smaller radius crystal. In actual x-ray laser experiments, the Ly-α lines may be blended together, as observed near the surface of the target, thereby making for an excellent resonance.

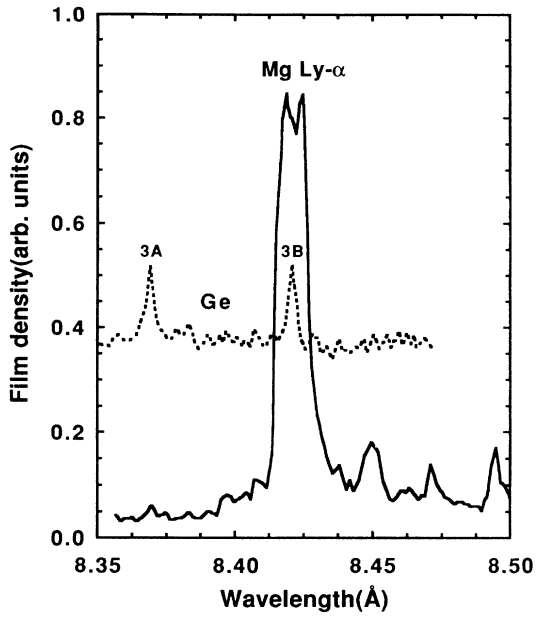

FIG. 5. Spectra of Mg and Ge plasmas measured in the coronal region by a curved crystal spectrograph with $R = 250$ mm in the FSSR geometry. Plasmas were produced at the NPO VNIIFTRI laser facility.

IV. PLT MEASUREMENTS

A third set of measurements was performed on the Princeton Large Torus (PLT) tokamak [24]. These measurements serve to illustrate the difficulties of measuring line $3B$ in an over-ionized plasma because of blending with transitions from the O-like Ge.

The PLT plasmas were 80 cm in diameter with a central electron temperature of 1.5 keV and a central electron density of about 3×10^{13} cm^{-3}. Because of the large plasma volume a Bragg-crystal spectrometer in the Johann configuration was used [24]. For the present measurement, the spectrometer employed a $100\times20\times0.5$ mm^3 ammonium dihydrogen phosphate (ADP) crystal with a lattice spacing of $2d = 10.648$ Å. The crystal was bent to a 57.3-cm radius and positioned for a nominal Bragg angle $\theta = 54.7°$. The analyzed x rays were detected with a microchannel-plate-intensified photodiode array. A detailed description of the instrument and its positioning on the PLT tokamak are given in Ref. [25].

Mg and Ge were alternately injected into PLT plasmas with the laser-ablation technique [26,27]. The quantities were kept low so as to not perturb the electron temperature. Injection took place at $t = 750$ ms after initiation of the discharge and 200 ms before the end of the discharge. A total of 48 spectra were recorded per discharge with 4-

ms time resolution; six of these spectra were recorded just before injection and served to monitor the line emission from elements indigenous to PLT plasmas. Following injection, strong radiation from Mg or Ge was observed for a period of about 50 ms. The spectra resulting from summing the data from five discharges with Ge injection and three discharges with Mg injection and covering the wavelength region 8.34–8.49 Å are shown in Fig. 6. The relatively high background level is due to Bremsstrahlung and continuum emission. Line emission from indigenous plasma impurities in this wavelength region consists mainly of the $n=4$ and $5\rightarrow n=2$ emission from Li-like through C-like iron [28]. This line emission, however, was insignificant compared to the Ge or Mg lines, and only one weak iron line, a $4s\rightarrow 2p$ transition in Li-like Fe at 8.376 Å could be distinctly identified. The measurements were calibrated by using several hydrogenic reference lines to establish the absolute wavelength scale and the spectral dispersion. To augment the reference standard given by the Mg Ly-α lines, Na was injected into four discharges, and the Ly-β and Ly-γ lines of H-like Na were recorded and set to the values of 8.459 50 and 8.021 07 Å, respectively, given by Garcia and Mack [17].

As a result of the rather high electron temperature Ge is ionized well beyond the Ne-like state. As seen from Fig. 6, the Ne-like lines $3A$ and $3B$ are accompanied by a large number of lines, most of which are attributed to transitions in O-like Ge. In fact, the most prominent line in the spectrum is attributed to the strong $2p\rightarrow 3d$ line in O-like Ge identified in the EBIT measurements. While line $3A$ appears unaffected by blends with the O-like Ge lines, line $3B$, whose intensity should be about half of that of $3A$, is almost completely obscured by the presence of the O-like $2p\rightarrow 3d$ line. Its location is indicated in Fig. 6 relative to that of $3A$ by using the 9.3-eV value of the theoretical splitting of the two lines. Close inspection of the data reveals a small shoulder on the long-wavelength side of the O-like Ge line. Attributing the shoulder to $3B$ and fitting the blend with Gaussian line shapes we find 8.4180 Å±0.7 mÅ (1472.85±0.13 eV) for the O-like Ge line and 8.425 Å±2 mÅ(1471.62±0.35 eV) for the Ne-like Ge line $3B$. The accuracy with which the wavelength of the O-like Ge line was measured exceeds that of the EBIT measurement and there is good agreement, 0.8 mÅ, between the two measurements. By contrast, the accuracy of $3B$ is much lower as a result of the difficulty in resolving $3B$ from the O-like line. A higher accuracy for $3B$ could be achieved if Ge were injected into a plasma with lower electron temperature (<1.0 keV) and assuming the absence of higher charge states than Ne-like Ge. The measurement of $3B$ differs from the EBIT and VNIIFTRI measurements by 3–4 mÅ. There may be more than two lines blended together due to satellite lines or other nearby O-like lines, in which case the measurement of line $3B$ is more uncertain and should not be relied upon. The PLT measurements point out the difficulty of identifying lines when there are blends, something which is quite common in spectroscopy. A small contribution of the O-like line in a somewhat colder plasma would have been particularly deceptive, shifting the measured value of the apparent line $3B$ without clearly indicating its presence.

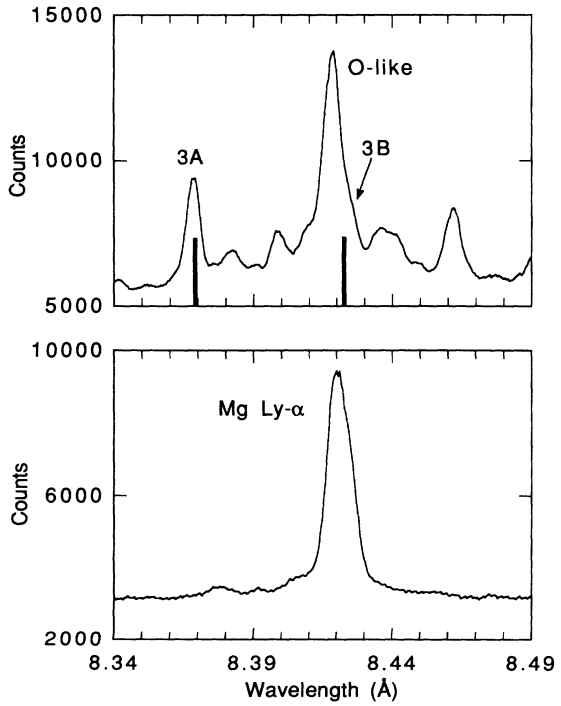

FIG. 6. Spectra of Mg and Ge plasmas measured on the PLT tokamak with central electron temperature of 1.5 keV and central electron density of 3×10^{13} cm^{-3}. The Ge line $3B$ is obscured by the strong O-like Ge line at 8.418 Å.

V. COMPARISON WITH OTHER MEASUREMENTS

Measurements 15 years ago measured the Ge $3B$ line at 8.423 Å±3 mÅ [29] and 8.427±5 mÅ [30] and more recently it was measured at 8.4237 Å±0.2 mÅ [31]. There are also very recent unpublished experiments, again in laser produced plasmas, which measure the Ge $3B$ line at 8.4216 Å±1.4 mÅ [32]. Given the large uncertainties in the first two measurements they are consistent with our measurements. However, the third measurement in Ref. [31] disagrees with the EBIT measurements by 1.8 mÅ and 2.9 mÅ and with the laser produced plasma experiments at VNIIFTRI by 2.8 mÅ and 2.9 mÅ. Both comparisons lie outside the uncertainty in the measurements and suggest that there may be a problem with this third measurement, which used a monolithic crystal as an absolute reference. The fourth measurement is in good agreement with the EBIT and VNIIFTRI measurements presented in this paper. A weighted arithmetic mean value of all the measurements summarized in Table I yield a value of 8.4232 Å for line $3B$. This is heavily weighted by Ref. [31]. If Ref. [31] is excluded, the weighted mean value is 8.4213 Å which compares well with a weighted mean value of 8.4210 Å for the EBIT and VNIIFTRI measurements presented in this paper. Regarding the relative intensities of Ge lines $3A$ and $3B$, the EBIT ratio is 2:1, which is consistent with EBIT measurements for other Ne-like ions, while the VNIIFTRI ratio is 1:1, which is also consistent with the ratio ob-

TABLE I. Measured and calculated values of the Ne-like Ge line $3B$, the ground state to $\overline{2s}_{1/2}3p_{1/2}$ ($J=1$) transition.

Measurement	Crystal (order)	Photon energy (eV)	Wavelength (Å)
EBIT	TlAP (2nd)	1472.16(18)	8.4219(10)
EBIT	ADP(1st)	1472.35(14)	8.4208(8)
VNIIFTRI	mica (100 mm) (2nd)	1472.36(16)	8.4208(9)
VNIIFTRI	mica (250 mm) (2nd)	1472.34(14)	8.4209(8)
PLT	ADP (1st)	1471.62(35)	8.425(2)
Boiko (Ref. [29])	mica (2nd)	1472.0(5)	8.423(3)
Gordon (Ref. [30])	mica (2nd)	1471.3(9)	8.427(5)
Rode (Ref. [31])	quartz (1st)	1471.85(3)	8.4237(2)
Dunn (Ref. [32])	ADP (1st)	1472.22(24)	8.4216(14)
Calculation	Method	Photon energy (eV)	Wavelength (Å)
MCDF	AL	1474.11	8.4109
MCDF	OL	1473.84	8.4124
MCDF	OL+CK+GS	1473.25	8.4158
MCDF	OL+CK+GS+MZ	1472.77	8.4185
Ref. [35]	MZ	1473.21	8.4159
Ref. [36]	RPTMP	1472.51	8.4199
Reference lines	Material	Photon energy (eV)	Wavelength (Å)
Ly-α_1	Mg	1472.64	8.4192
Ly-α_2	Mg	1471.69	8.4246

served in other Ne-like ions in laser produced plasmas [29].

VI. CALCULATIONS OF Ge LINES

The calculation of the energies and the wavelengths of the $2s \rightarrow 3p$ transitions in Ne-like Ge was performed using the MCDF atomic physics code of Grant and coworkers [19]. The code uses several different methods to optimize the wave functions used in the energy calculation. The two methods discussed here are referred to as the average level (AL) mode and the optimal level (OL) mode. The first method (AL) is optimized for a weighted average energy of all the levels considered while the second (OL) optimizes the wave functions for a given level or group of levels. In both modes, the energy of the Ne-like ground state was calculated in a separate run from the energies of the 36 $n=3$ excited states and subtracted to obtain the transition energy. For the AL calculations we obtain a value of 1474.11 eV for the Ge $3B$ line. When the OL calculations are optimized for the excited levels of lines $3A$ and $3B$ the energy is lowered by 0.27 eV for line $3B$. If we then include interactions with the states $\overline{2p}\,\overline{2p}3p3d$ ($J=1$), which involve Coster-Kronig (CK) fluctuations, in the OL calculation of the $2s_{1/2}3p_{1/2}$ ($J=1$) level as well as ground-state correlation (GS) energy which arises from breaking pairs in the closed core, then the energy is lowered by 0.86 eV for line $3B$ as compared with the AL calculation resulting in a wavelength of 8.4158 Å. This assumes a 1.0-eV correlation energy as described in Ref. [33]. We then use the theoretical values of the first- and second-order Z-expansion (MZ) correlation energies [34] relative to the ground state correlation energy to make a final correction to the energy. This results in a value of 8.4185 Å for the $3B$ line.

Other recent calculations reported in the literature have obtained values for the wavelength of the $3B$ line of 8.4159 Å [35] using the Z-expansion method (MZ) and 8.4199 Å [36] using the relativistic perturbation theory with a model potential (RPTMP). All the calculations are less than the measured wavelengths discussed above by 1–10 mÅ. This is consistent with previous experiments on Ne-like ions which show that the calculated wavelengths are less than the measured wavelengths for transitions involving a $2s$ hole in the closed L shell. The measured and calculated values of the Ne-like Ge line $3B$ are summarized in Table I. The difficulty of calculating the energy of the $3B$ line (or any Ne-like transition) to an accuracy better than about one part per thousand points out the need for accurate measurements.

VII. CONCLUSIONS

We have measured the wavelength of the ground state to $\overline{2s}_{1/2}3p_{1/2}$ ($J=1$) transition in Ne-like Ge, referred to as line $3B$, relative to the Ly-α line of Mg. The measurements were done by three different approaches and are compared with previous experimental measurements and current calculations. The EBIT and VNIIFTRI measurements yield a weighted mean value of 8.4210 Å for this line which lies between the two components of the Ly-α line of Mg. In particular, it differs 1.8 mÅ from Ly-α_1 and 3.6 mÅ from Ly-α_2, or 210 and 430 ppm, respectively, and thus appears to be a good resonance for potential use in a resonantly photo-pumped laser scheme.

We also measured the wavelength of a $2p \rightarrow 3d$ transition in O-like Ge with EBIT and PLT and obtain a weighted mean value of 8.4182 Å. This line lies very close to the position of the Ne-like Ge line, and we discussed how a blend of these two lines could shift the measured position of the Ne-like Ge line if care is not made to distinguish the two features.

ACKNOWLEDGMENTS

The authors wish to thank the National Scientific and Research Institute for Physical-technical and Radiotechnical Measurements (NPO VNIIFTRI), Russia, the P. N. Lebedev Physical Institute of the Russian Academy of Sciences, the National Institute of Technical Physics, Russia, and Lawrence Livermore National Laboratory, USA, which have allowed this collaboration. The authors would like to thank James H. Scofield for advice during preparation of this manuscript and the staff of the PLT facility at the Princeton Plasma Physics Laboratory for support, with special thanks to Tom Gibney. The work of the LLNL authors was performed under the auspices of the U.S. Department of Energy by Lawrence Livermore National Laboratory under Contract No. W-7405-ENG-48.

[1] R. C. Elton, *X-ray Lasers* (Academic Press, San Diego, 1990), pp. 99–198.
[2] C. H. Skinner, Phys. Fluids B **3**, 2420 (1991).
[3] B. J. MacGowan, L. B. DaSilva, D. J. Fields, C. J. Keane, J. A. Koch, R. A. London, D. L. Matthews, S. Maxon, S. Mrowka, A. L. Osterheld, J. H. Scofield, G. Shimkaveg, J. E. Trebes, and R. S. Walling, Phys. Fluids B **4**, 2326 (1992).
[4] P. Beiersdorfer, J. Nilsen, A. Osterheld, D. Vogel, K. Wong, R. E. Marrs, and R. Zasadzinski, Phys. Rev. A **46**, R25 (1992).
[5] S. Elliott, P. Beiersdorfer, and J. Nilsen, Phys. Rev. A **47**, 1403 (1993).
[6] J. Nilsen, P. Beiersdorfer, S. R. Elliott, and A. L. Osterheld, Phys. Scr. **47**, 42 (1993).
[7] K. Gäbel, Ch. Bergmann, E. Fill, E. Förster, and I. Uschman, Appl. Phys. B **56**, 3 (1993).
[8] V. Yu. Politov and M. K. Shinkarev, Pis'ma Zh. Eksp. Teor. Fiz. **58**, 794 (1993) [JETP Lett. **58**, 740 (1993)].
[9] V. Yu. Politov, P. A. Loboda, V. A. Lykov, and Joseph Nilsen, Opt. Commun. **108**, 283 (1994).
[10] R. E. Marrs, M. A. Levine, D. A. Knapp, and J. R. Henderson, Phys. Rev. Lett. **60**, 1715 (1988).
[11] M. A. Levine, R. E. Marrs, J. N. Bardsley, P. Beiersdorfer, C. L. Bennett, M. H. Chen, T. Cowan, D. Dietrich, J. R. Henderson, D. A. Knapp, A. Osterheld, B. M. Penetrante, M. B. Schneider, and J. H. Scofield, Nucl. Instrum. Methods Phys. Res. Sect. B **43**, 431 (1989).
[12] P. Beiersdorfer and B. J. Wargelin, Rev. Sci. Instrum. **65**, 13 (1994).
[13] I. G. Brown, J. E. Galvin, R. A. MacGill, and R. T. Wright, Appl. Phys. Lett. **49**, 1019 (1986).
[14] W. R. Johnson and G. Soff, At. Data Nucl. Data Tables **33**, 405 (1985).
[15] J. Nilsen, J. H. Scofield, and E. A. Chandler, Appl. Opt. **31**, 4950 (1992).
[16] G. W. Erickson, J. Phys. Chem. Ref. Data **6**, 831 (1977).
[17] J. D. Garcia and J. E. Mack, J. Opt. Soc. Am. **55**, 654 (1965).
[18] V. A. Boiko, V. G. Palchikov, I. Yu. Skobelev, and A. Ya. Faenov, *Spectroscopic Constants of Atoms and Ions: Spectra of Atoms With One and Two Electrons* (Standart, Moscow, 1988).
[19] I. P. Grant, B. J. McKenzie, P. H. Norrington, D. F. Mayers, and N. C. Pyper, Comput. Phys. Commun. **21**, 207 (1980).
[20] B. A. Bryunetkin, G. V. Ivanekov, S. A. Pikuz, A. Ya. Faenov, T. A. Shelkovenko, Pis'ma Zh. Tekh. Fiz. **17**(19), 24 (1991) [Sov. Tech. Phys. Lett. **17**, 689 (1991)].
[21] B. A. Bryunetkin, S. A. Pikuz, I. Yu. Skobelev, and A. Ya. Faenov, Lasers Particle Beams **10**, 849 (1992).
[22] B. A. Bryunetkin, I. Yu. Skobelev, A. Ya. Faenov, M. P. Kalashnikov, P. Nickles, M. Schnürer, and S. A. Pikuz, Quantum Electron. **23**, 337 (1993).
[23] B. A. Bryunetkin, S. A. Pikuz, I. Yu. Skobelev, A. Ya. Faenov, B. K. Khabibulaev, and Sh. A. Ermatov, Kvant. Elektron. (Moscow) **19**, 916 (1992) [Sov. J. Quantum Electron. **22**, 853 (1992)].
[24] P. Beiersdorfer, Ph.D. thesis, Princeton University, 1988 (unpublished), available from University Microfilms, Ann Arbor, MI, Order No. 8812108.
[25] P. Beiersdorfer, S. von Goeler, M. Bitter, K. W. Hill, R. A. Hulse, and R. S. Walling, Rev. Sci. Instrum. **60**, 895 (1989).
[26] E. S. Marmar, J. L. Cecchi, and S. A. Cohen, Rev. Sci. Instrum. **46**, 1149 (1975).
[27] J. Timberlake, S. Cohen, C. Daughney, and D. Manos, J. Vac. Sci. Technol. A **1**, 841 (1983).
[28] B. J. Wargelin *et al.* (unpublished).
[29] V. A. Boiko, A. Ya. Faenov, and S. A. Pikuz, J. Quant. Spectros. Radiat. Transfer **19**, 11 (1978).
[30] H. Gordon, M. G. Hobby, N. J. Peacock, and R. D. Cowan, J. Phys. B **12**, 881 (1979).
[31] A. V. Rode, A. M. Maksimchuk, G. V. Sklizkov, A. Ridgeley, C. Danson, N. Rizvi, R. Bann, E. Forster, K. Goetz, and I. Uschmann, J. X-ray Sci. Technol. **2**, 149 (1990).
[32] Jim Dunn (unpublished).
[33] P. Beiersdorfer, S. von Goeler, M. Bitter, E. Hinnov, R. Bell, S. Bernabei, J. Felt, K. W. Hill, R. Hulse, J. Stevens, S. Suckewer, J. Timberlake, A. Wouters, M. H. Chen, J. H. Scofield, D. D. Dietrich, M. Gerassimenko, E. Silver, R. S. Walling, and P. L. Hagelstein, Phys. Rev. A **37**, 4153 (1988).
[34] U. I. Safronova and V. S. Senashenko, *Theory of Spectra of Multicharged Ions* (Energoatomizdat, Moscow, 1984).
[35] E. V. Aglitskii, E. P. Ivanova, S. A. Panin, U. I. Safronova, S. I. Ulityn, L. A. Vainshtein, and J. F. Wyart, Phys. Scr. **40**, 601 (1989).
[36] E. P. Ivanova and A. V. Gulov, At. Data Nucl. Data Tables **49**, 1 (1991).

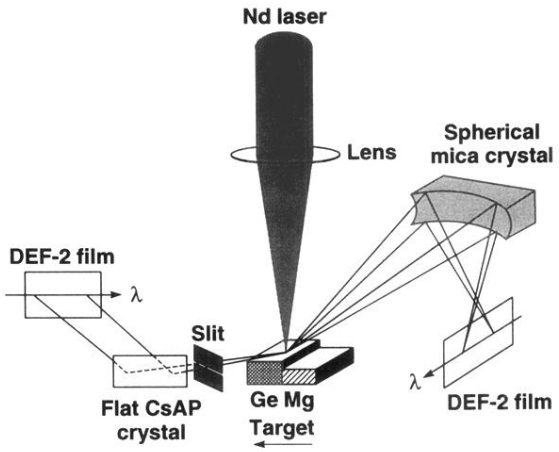

FIG. 4. Experimental geometry for the spectral measurements done at the NPO VNIIFTRI laser facility. A Nd laser illuminates a Ge or Mg target. Spectra are recorded with flat and curved crystal spectrographs. The curved crystal spectrograph uses the geometry of the focusing spectrograph with spatial resolution (FSSR).